HYPER-SPECTRAL IMAGING OF BIOFILM GROWTH DYNAMICS

Lubos Polerecky, Judith M. Klatt, Mohammad Al-Najjar, Dirk de Beer

Max-Planck Institute for Marine Microbiology, Celsiusstrasse 1, 28359 Bremen, Germany

ABSTRACT

Spectrally resolved imaging was applied to study the growth dynamics of phototrophic biofilms comprizing a mixture of one cyanobacterial and one diatom species. Linear spectral unmixing was combined with liquid chromatography to quantitatively discriminate the areal biomass densities of the two populations. The grown biofilms exhibited highly heterogeneous distribution with patches of 1–2 mm in size, although the conditions provided for growth, including substrate roughness, illumination and flow of the overlying water, were homogeneous. The biomass was initially dominated by cyanobacteria, which exhibited an exponential-like growth phase during days 2–7. Their population declined during days 9–17, which coincided with the growth phase of the diatom population. By allowing non-invasive and real-time measurements and data evaluation, the spectral imaging approach constitutes a useful tool for microbial ecologists.

Index Terms— Biofilm, Phototroph, Population dynamics, Spectral imaging

1. INTRODUCTION

Benthic phototrophic biofilms constitute a signifficant source of organic carbon in shallow-water and intertidal habitats, and represent sites of intensive nutrient cycling with major impacts on ecosystem functioning [1]. Quantification of their biomass with a high temporal and spatial resolution is therefore required to understand the ecology and aid the management of coastal areas. Over the past decade, measurements of spectral reflectance have been increasingly applied for this purpose, especially because of their potential for rapid assessment over large areas. For example, methods have been developed for the classification of sediments based on their basic characteristics, e.g., water content or median grain size, or for the quantification of the sedimetary pigment content as a proxy for the microphytobenthic biomass [2, 3, 4].

To understand the processes of attachment, detachment and growth, many studies have investigated the biofilm structure, physiology of the community members and the dynamics of physico-chemical parameters in biofilms [5, 6, 7, 8]. In this study we aimed to develop a hyper-spectral imaging approach as a tool for rapid and non-invasive monitoring of actively growing biofilms. We especially aimed to test whether the approach allows *discrimination* between different members of the biofilm microbial community and a *quantitative* assessment of their growth dynamics. Our approach employs hyperspectral imaging of the biofilm's reflectance with a high spectral resolution ($\approx$ 2 nm). The discrimination of the members in the mixed biofilm population was achieved through a linear unmixing of the log-transferred reflectance spectra into end-members, each associated with a specific group of cells. The quantification was based on a relationship between the pigment content determined by liquid chromatography and the magnitude of the end-member spectra, which was determined separately for each community member and validated using mixed cell populations with known compositions.

We are grateful for the financial support provided by European Commission (project ECODIS, project number 518043), the Yusef Jameel foundation and the Max-Planck Society. We thank Dr. Andrew Bissett and Dr. Martin Beutler for their assistance and helpful discussions.

2. MATERIALS AND PROCEDURES

Biofilms were grown on white substrates placed in two independent flow-through chambers. The substrate surface had a matt (diffusive) finish, achieved by filing the originally glossy surface with a fine sandpaper. An artificial sea-water medium with added nutrients and silicate was let flow through the flow-cells at a velocity of about 1 cm s^{-1}, and the substrates were homogeneously illuminated in 12 h light and 12 h dark intervals with photosyntetically active radiation (400–700 nm, intensity 50 μmol photons m^2 s^1).

On day zero, the medium was inoculated with a mixed suspension of diatom (*Cylindrotheca closterium*) and cyanobacterial (*Synechococcus elongates*) cells. On day one, the medium was exchanged to prevent suspended cells from interfering with the measurements of the cells colonizing the substrate. On day 17, one of the substrates from each flow-chamber was cleaned. From this day, the illumination of half of the substrates in each flow-chamber was decreased to $\sim$ 20 % of the original intensity by covering the target area with a semi-transparent foil. The shaded area was next to the inlet and outlet of the first and second chamber, respectively.

The modular spectral imaging (MOSI) system developed recently [9] was used to acquire images of spectral reflectance, $R(\lambda)$ from the biofilms. The hyperspectral camera (Pika, Resonon; detection range 420–870 nm with $\approx$ 2 nm

resolution) was placed at a distance of about 40 cm above the biofilms and was attached to an x–y linear positioning stage (VT-80, Micos), which allowed reproducible scanning of the biofilm surface. Illumination in the range 400–800 nm was provided by a halogen bulb (Philips), which was attached next to the objective lens of the camera. The incubation light source was temporarily (for 5–10 min) switched off during scanning. Hyper-cube analysis was done as previously described [9], using software HS_ImAn available at WWW.MICROSEN-WIKI.NET.

The MOSI system was calibrated using artificially prepared biofilms of known microalgal contents. First, pure cultures of cyanobacteria and diatoms were diluted in their respective growth media and mixed with agarose with low melting temperature. The mixtures of pure cells were then poured into a micro-chamber constructed from two microscope glass slides separated with a 1 mm spacer. After solidifying, the biofilms were placed onto the same white subtrate as those used during the growth experiment and scanned with the MOSI system. The log-transfered reflectance spectra obtained by this procedure were defined as end-member spectral vectors in the multi-dimensional λ-space, $\vec{v}_x$, with components $v_{x,i} = \log R_x(\lambda_i)$, $i = 1, \ldots, N$, where $x = c$ stands for cyanobacteria, $x = d$ for diatoms, and N is the total number of imaged spectral bands (here $N = 150$). Subsequently, the areal contents of the common (Chl a) and group-specific (fucoxanthin for diatoms, zeaxanthin for cyanobacteria) photopigments in the artificial biofilms were quantified by high performance liquid chromatography (HPLC). The calibration was derived separately for cyanobacteria and diatoms by plotting the magnitudes of the respective end-member spectral vectors $\vec{v}_c$ and $\vec{v}_d$ against the pigment contents determined by HPLC.

To validate the calibration for mixed biofilms, the same procedure was repeated for artificial biofilms prepared from arbitrarily chosen mixtures of cyanobacterial and diatom cells. First, the reflectance spectra of the mixed biofilms, $\log R_m(\lambda)$, were measured and linearly decomposed into a sum of the group-specific spectra, i.e., $\log R_m(\lambda) = a_c\vec{v}_c(\lambda) + a_d\vec{v}_d(\lambda)$. Then, the calibration plots $|\vec{v}_c|$ vs. [Chl a]$_c$ and $|\vec{v}_d|$ vs. [Chl a]$_d$ determined from the pure culture measurements were used to calculate the cyanobacterial and diatom contents. Finally, these values were compared with those determined by HPLC, derived from the measured contents of Chl a and the group-specific accessory pigments.

3. RESULTS

3.1. Calibration and validation

Reflectance spectra of the artificial cyanobacterial and diatom biofilms used for the calibration were sufficiently distinct to allow reliable discrimination of their respective contributions to the spectra in mixed biofilms (Fig. 1A). When plotted in a log-log scale, areal densities of the measured pigments for both species varied linearly with the magnitudes of the log-transformed spectral reflectance spectra (expressed as the length of the spectral vectors $\vec{v}_c$ and $\vec{v}_d$; Fig. 1B). As expected, the slopes of these plots were equal for the pigments belonging to the given species, consistent with the fact that the ratio between the pigments was independent of the dilution factor with which the artificial biofilms were prepared. On the other hand, the slopes of the calibration plots differed between the two studied species (1.178 for cyanobacteria, 1.38 for diatoms; Fig. 1B) as well as differed from 1, possibly due to light scattering that caused the amount of light absorbed in the biofilm to increase faster with the increasing cell content than would be expected without scattering. The minimum detectable areal Chl a content was about 0.01 mg cm^{-2}.

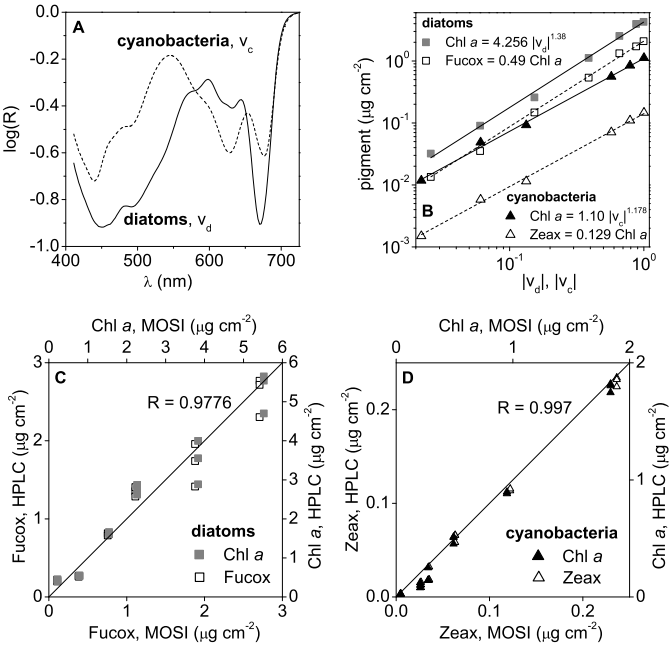

Fig. 1. Calibration and validation of the pigment analysis based on hyper-spectral imaging of spectral reflectance. Lengths of the shown end-member spectra for the studied species (A) were set equal to unity ($|\vec{v}_c| = |\vec{v}_d| = 1$). (B) Relationships between areal densities of the common (Chl a) and group-specific (Fucoxanthin and Zeaxanthin) pigments and the lengths of the spectral vectors $\vec{v}_c = \log R_c(\lambda)$ and $\vec{v}_d = \log R_d(\lambda)$, derived from the meaurements on pure-culture biofilms. (C–D) Plots of areal pigment densities calculated from the hyper-spectral signals against those quantified by HPLC, derived from the measurements on mixed biofilms.

When tested with artificial biofilms comprizing a mixture of cells, the pigment contents associated with the two species that were derived from the hyper-spectral measurements reproduced very well the corresponding pigment contents mea-

sured directly with HPLC (Fig. 1C–D), validating the applicability of the spectral imaging approach for non-invasive pigment quantification.

3.2. Population dynamics

The substrate colonization by cyanobacteria was initially homogeneous, although a few streak-like areas with increased cell densities were also observed (Fig. 2B). A closer inspection revealed that these areas were located downstream from small protrusions on the substrate, which resulted in locally enhanced velocities of the water flow above the substrate. The distribution of cyanobacteria became patchy after several days, when diatom abundance increased (Fig. 2E & H). In contrast, substrate colonization by diatoms started off in distinct clusters of 1–2 mm in size (Fig. 2C & F), which progressively grew and eventually merged into a more homogeneous coverage (Fig. 2I).

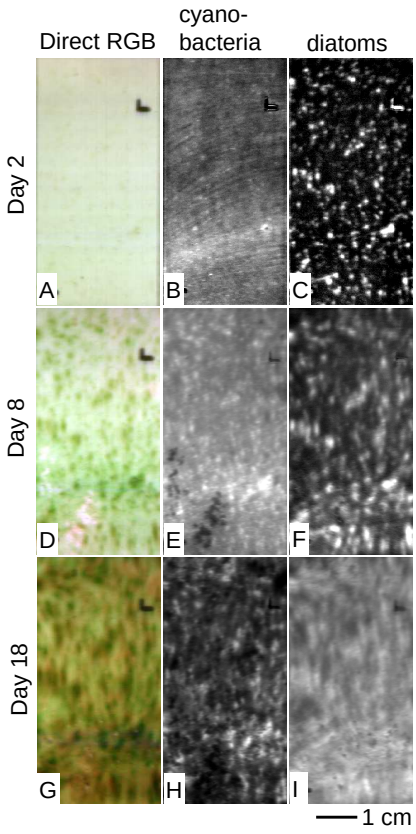

Fig. 2. Examples of direct RGB images and distributions of cyanobacteria and diatoms in the biofilm at different growth stages (days after inoculation). One substrate is shown. The gray scale and contrast of the shown images were altered to improve visualization of the features discussed in the text. Brigther areas represent higher biomass densities. Water flow direction was from left to right.

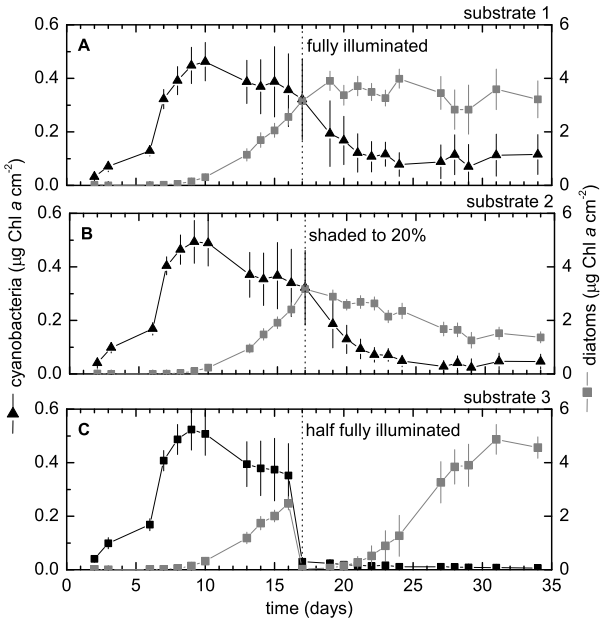

Fig. 3. Dynamics of cyanobacterial and diatom populations, expressed as areal density of Chl a, on three selected substrates. Error-bars represent spatial variability of the biomass over the substrate and indicate the level of patchiness. Substrate 3 was cleaned on day 17, and only the biomass on the fully illuminated half is shown. Note different scales for the cyanobacterial and diatom biomass.

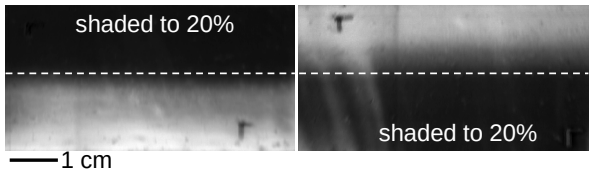

Fig. 4. Distributions of diatoms on substrates from two replicate flow chambers, 8 days after the substrates were cleaned. Half of each substrate was shaded, as indicated with the dashed line. Water flow direction was from bottom to top. Brigther areas represent higher biomass densities.

Cyanobacteria started to form detectable biofilms within 2 days after inoculation, with an exponential-like growth phase occurring between days 2–7 (doubling time ~ 12 h; Fig. 3). In contrast, diatoms coverage exhibited a lag phase of 6 days, followed by an exponential growth phase during days 6–10 (doubling time $\sim$27 h; Fig. 3). From day 10, the diatom abundance increased approximately linearly and was accompanied by a gradual decrease in the cyanobacterial biomass. These temporal dynamics as well as the magnitudes of the biomass densities were similar for all substrates in both flow-through chambers (not shown).

After day 17, when the illumination of half of the substrates was decreased to $\sim$ 20 %, the pronounced but gra-

dual decrease in the cyanobacterial biomass continued, with a similar initial rate for all substrates. The diatom biomass remained at its maximum level on the fully illuminated substrates, whereas it gradually decreased on the shaded ones. Interestingly, approximately from day 27 the areal coverage of the shaded substrates was about half of the fully illuminated ones, which was observed for both cyanobacteria and diatoms (Fig. 3).

The substrate that was cleaned on day 17 became re-colonized with diatoms but not with cyanobacteria (Fig. 3C). The biofilm exhibited similar growth phases as that observed for the initial colonization. However, in contrast to the initial colonization, the coverage of the re-colonized substrate was not patchy but rather homogeneous in the direction perpendicular to the water flow and gradualy decreasing downstream of the flow (Fig. 4). Irrespective of the water flow direction, the biomass density on the fully illuminated half of the substrate was much larger than on the shaded one.

4. DISCUSSION

We have demonstrated that the spectral imaging approach allows truly quantitative characterization of the biofilm microbial composition. This was allowed primarily by the fact that the spectral signatures of the cells comprizing the biofilm were distinct. Unlike traditional techniques based on pigment extraction, such as HPLC, the spectral imaging approach is non-invasive, very simple, and allows sensitive pigment quantification with high spatial and temporal resolution. Furthermore, it can easily be combined with other non-invasive and high spatial resolution methods, such as microsensors, to correlate the structural information with the measurements of physico-chemical parameters and metabolic activity. Thus, it is a valuable tool for physiological studies of microbial populations in actively growing biofilms.

Admittedly, the calibration procedure is rather time-consuming, as it requires HPLC-based pigment quantification in several samples with pigment contents covering a range of at least 2 orders of magnitude. However, the advantage is that once the spectral imaging system is calibrated and the calibration procedure is validated, many samples can be analysed with very little effort.

Due to the fact that the technique is based on spectral imaging, i.e., the detection of color, it is applicable only for pigmented members of the studied microbial communities. The confidence of the separate quantification of single community members in a mixed population depends on the differences in their spectral signatures. Spectral imaging in a large number of bands is required to enable quantitatively reliable discrimination of multiple species or functional groups.

In the case study, we have demonstrated a possible use of the spectral imaging approach for monitoring of the population dynamics of cells forming a complex biofilm. We showed how differently cyanobacteria and diatoms colonize the substrates, both in time and space, and how they interact with and compete against each other during the different stages of the biofilm development.

5. REFERENCES

[1] L. B. Cahoon, "The role of benthic microalgae in neritic ecosystems," *Oceanography and Marine Biology: an Annual Review*, vol. 37, pp. 47–86, 1999.

[2] J.-P. Combe, P. Launeau, V. Carrere, D. Despan, V. Meleder, L. Barille, and C. Sotin, "Mapping microphytobenthos biomass by non-linear inversion of visible-infrared hyperspectral images," *Remote Sensing of Environment*, vol. 98, no. 4, pp. 371–387, 2005.

[3] B. Deronde, P. Kempeneers, and R.M. Forster, "Imaging spectroscopy as a tool to study sediment characteristics on a tidal sandbank in the westerschelde," *Estuarine, coastal and shelf science*, vol. 69, no. 3–4, pp. 580–590, 2006.

[4] J. C. Kromkamp, E. P. Morris, R. M. Forster, C. Honeywill, S. Hagerthey, and D. M. Paterson, "Relationship of intertidal surface sediment chlorophyll concentration to hyperspectral reflectance and chlorophyll fluorescence," *Estuaries and coasts*, vol. 29, no. 2, pp. 183–196, 2006.

[5] M. W. Mittelman, "Structure and functional characteristics of bacterial biofilms in fluid processing operations," *J Dairy Sci*, vol. 81, pp. 2760–2764, 1998.

[6] J. D. Bryers, "Processes contributing to biofilm formation: A review," in *First International Conference on Fixed Film Biological Processes*, YC Wu et al., Ed., Kings Island, Ohio, 1982, pp. 155–18.

[7] T. J. Battin, Kaplan L. A., Newbold J. D., Cheng X. H., and Hansen C., "Effects of current velocity on the nascent architecture of stream microbial biofilms," *Appl Environ Microb*, vol. 69, pp. 5443–5452, 2003.

[8] C. Barranguet, van Beusekom S. A. M., Veuger B., Neu T. R., Manders E. M. M., Sinke J. J., and Admiraal W., "Studying undisturbed autotrophic biofilms: still a technical challenge," *Aquat Microb Ecol*, vol. 34, pp. 1–9, 2004.

[9] L. Polerecky, A. Bissett, M. Al Najjar, P. Faerber, H. Osmers, P. Suci, P. Stoodley, and D. de Beer, "Modular spectral imaging (MOSI) system for discrimination of pigments in cells and microbial communities," *Applied and Environmental Microbiology*, vol. 75, no. 3, pp. 758–771, 2009.